JOURNAL OF SOLID STATE CHEMISTRY **98**, 174–180 (1992)

$CaNb_2P_2O_{11}$: A New Calcium Niobium (V) Oxophosphate with a Quasi-One-Dimensional Structure

DEBORAH L. SERRA AND SHIOU-JYH HWU*

Department of Chemistry, Rice University, P.O. Box 1892, Houston, Texas 77251

Received October 11, 1991; in revised form November 18, 1991

The crystal structure of a new calcium niobium (V) oxophosphate, $CaNb_2P_2O_{11}$, has been determined by single crystal X-ray diffraction. The title compound crystallizes in the monoclinic crystal system with the space group $C2/c$ (No. 15) and $Z = 4$. The lattice parameters are $a = 14.930$ (3) Å, $b = 10.824$ (3) Å, $c = 5.214$ (2) Å, $\beta = 93.59$ (2) Å, and $V = 840.9$ (4) Å^3. The structure contains a double layer of zig-zag corner-sharing NbO_6 octahedral chains. These octahedral chains are structurally isolated by PO_4 tetrahedral groups, each of which shares three oxygen atoms with NbO_6 octahedra to form a quasi-low-dimensional network structure. The interconnected octahedral chains are arranged parallel to each other so that channel structures are formed. The fourth oxygen atoms of the PO_4 tetrahedra are pointing into the channel where the calcium atoms are located. A structure comparison with the isotypic compound $BaNb_2P_2O_{11}$ and a discussion of the Nb–O framework formation related to that in the purple molybdenum bronze are presented. © 1992 Academic Press, Inc.

Introduction

Over the years much attention has been devoted to the reduced ternary and quaternary transition metal oxides that possess metal–insulator transitions. A number of interesting and technologically important physical phenomena are associated with metal–insulator transitions (*1–3*), such as superconductivity, charge density waves, and magnetic ordering. Structurally, the transition metal–oxygen–transition metal linkage is a common structure feature observed in these metal oxide frameworks and is deemed important to the transport properties which are induced by conduction electrons. However, electron–electron and electron–lattice interactions in metal oxides are not yet fully understood, due to the complex interactions that result from complicated solid-state, extended lattice frameworks. Compounds with quasi-low-dimensional structures, such as the bronzes (*3*), provide a simple structure for the possible study of the behavior of delocalized electrons in a confined space. Most oxide bronzes are formed in ternary systems with a general formula $A_xM_yO_z$ (A = electropositive elements, M = transition metals). Commonly, pseudo-one or two-dimensional transition metal oxide chains or layers are found to be separated by electropositive cations. Consequently these compounds possess anisotropic transport properties. However, the interchain or layer electron interaction often complicates the interpretation of physical phenomena. Incorporation of a closed-shell cation, such as P^{5+}, allows

---

* To whom correspondence should be addressed.

0022-4596/92 $5.00

frameworks that mimic bronze structures to form, e.g., $BaNb_3P_3O_{15}$ (*4*). During a recent attempt to synthesize the calcium analogue of this barium phase, we have isolated an oxophosphate compound with a mixed structure that consists of transition metal oxide octahedra which are structurally isolated by closed-shell phosphate groups. In this paper, we report the synthesis and structure of this newly prepared calcium niobium (V) oxophosphate, $CaNb_2P_2O_{11}$, and present a detailed structure comparison with the isotypic compound $BaNb_2P_2O_{11}$ (*5*). To discern the difference from the bronze structure in terms of the formation of mixed polyhedra, a structural relationship between the title compound and the purple molybdenum bronze $K_{0.9}Mo_6O_{17}$ (*6*) is discussed.

Experimental

Synthesis. Single crystals of $CaNb_2P_2O_{11}$ were grown at 1100°C from an oxide mixture with the composition $CaNb_3P_3O_{15}$. The sample was prepared in two steps. First, $CaNb_2O_6$ was synthesized by calcining a stoichiometric mixture of $CaCO_3$ (AESAR, 99.97%) and Nb_2O_5 (Aldrich, 99.99%) in air at 1000°C. The second step involved the addition of Nb metal, Nb_2O_5, and P_2O_5 to $CaNb_2O_6$ in a mole ratio of 4 : 3 : 15 : 10, respectively. The mixture was placed in an evacuated silica ampule and heated for 9 days at ca. 1100°C. After it was reground, the polycrystalline product was again heated at 1100°C for 10 days and allowed to cool in the furnace to room temperature. Dark rectangular gem crystals of the title compound were found along the bottom side of the ampule.

TABLE I

CRYSTALLOGRAPHIC DATA FOR $CaNb_2P_2O_{11}$

Formula mass (amu)	463.83
Space group	$C2/c$ (No. 15)
Cell parameters[a]	
a(Å)	14.930 (3)
b(Å)	10.824 (3)
c(Å)	5.214 (2)
β	93.59 (2)°
V (Å^3)	840.9 (4)
Z	4
T(K) of data collection	296 K
ρ calc. (g cm^{-3})	2.573
Radiation (graphite monochromated)	Mo$K\alpha$(λ = 0.71069 Å)
Crystal shape, color	Rectangular, dark blue
Crystal size (mm)	0.15 × 0.10 × 0.05
Linear abs. coeff. (cm^{-1})	25.6
Transmission factors	0.93–1.0
Scan type	ω-scan
Scan speed (deg min^{-1})	4.0
Scan range (deg)	-0.36 to 0.36 in ω
Background counts	¼ of scan range on each side of reflection
2θ (max)	55°
Data collected	$+h$, $+k$, $\pm l$
p for $\sigma(F^2)$	0.03
No. of unique data ($F_0^2 > 0$)	1015
No. of unique data with $F_0^2 > 3\sigma(F_0^2)$	827
F_{000}	880
$R(F^2)$	0.022
$R_w(F^2)$	0.030
R (on F for $F_0^2 > 3\sigma(F_0^2)$)	0.009
Goodness of fit	1.19
No. of variables	74

[a] The refinement of cell constants is constrained in the monoclinic crystal system.

Structure determination. Diffraction data were collected at room temperature on a Rigaku AFC5S four circle diffractometer. Crystallographic data for the title compound are summarized in Table I. The unit cell parameters and the orientation matrix for data collection were determined by a least-squares fit of 25 peak maxima with $8° < 2\theta < 28°$. There was no detectable decay during the data collection according to the intensities of three standard reflections ($1\,\bar{3}\,\bar{1}$; $0\,\bar{2}\,\bar{1}$; $\bar{4}\,\bar{2}\,\bar{1}$) which were measured every 150 reflections. The TEXSAN (*7*) software package was used for the crystal structure solution and refinement. Data reduction, intensity analysis, and space group determina-

TABLE II

POSITIONAL AND ISOTROPIC THERMAL PARAMETERS FOR $CaNb_2P_2O_{11}$

Atom	Wyckoff notation	x	y	z	B_{eq} (Å^2)[a]
Ca	4e	$\frac{1}{2}$	0.1066(1)	$\frac{1}{4}$	0.80(4)
Nb	8f	0.37519(2)	0.38030(3)	0.26153(7)	0.50(2)
P	8f	0.14748(6)	0.3326(1)	0.2456(2)	0.46(4)
O(1)	8f	0.1134(2)	0.0241(3)	0.4275(5)	0.8(1)
O(2)	4e	$\frac{1}{2}$	0.3351(4)	$\frac{1}{4}$	0.8(2)
O(3)	8f	0.2440(2)	0.3829(3)	0.2870(6)	0.9(1)
O(4)	8f	0.3816(2)	0.2145(3)	0.4938(5)	0.8(1)
O(5)	8f	0.1485(2)	0.2254(3)	0.0520(5)	1.0(1)
O(6)	8f	0.0844(2)	0.4313(3)	0.1357(6)	0.9(1)

[a] Isotropic equivalent thermal parameters defined as $B_{eq} = (8\pi^2/3)$ trace U, for those atoms refined using anisotropic displacement parameters.

tion were accomplished with the program PROCESS. On the basis of the intensity statistics as well as the successful solution and structure refinement, the space group was determined to be $C2/c$ (No. 15). Lorentz-polarization and empirical absorption corrections based on three azimuthal scans (2θ = 15.70°, 25.13°, 31.70°) were applied to the intensity data. The atomic coordinates were found using the program SHELXS-86 (*8*). The structural and thermal parameters were then refined by full-matrix least-squares methods and based on F^2 to R = 0.022, R_w = 0.030, and GOF = 1.19. The final positional and thermal parameters are given in Table II.

Structure Description and Discussion

In Fig. 1, the unit cell of the title compound is viewed approximately along the c axis. It shows that the structure is built up from clusters composed of four corner-sharing NbO_6 octahedra (drawn in thick lines) and isolated PO_4 phosphate groups (drawn in thin lines). The four octahedrally coordinated NbO_6, located around the body center of the unit cell, share four oxo oxygen atoms, 2 × O(1) and 2 × O(2), to form a Nb_4O_{20} unit. The neighboring Nb_4O_{20} units, centered around the c axis, are symmetry related by diagonal glide planes perpendicular to the b axis at $y = \frac{1}{4}$ and $\frac{3}{4}$. These Nb_4O_{20} units are interconnected by PO_4 groups us-

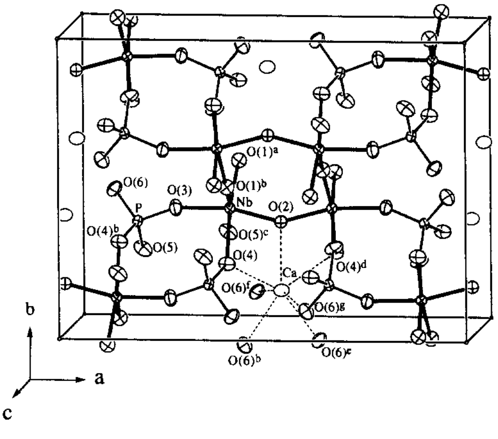

FIG. 1. An ORTEP drawing of the $CaNb_2P_2O_{11}$ structure viewed approximately along the c axis. The anisotropic atoms are presented in 90% probability. The NbO_6 octahedral coordination is shown in thick lines, while the PO_4 tetrahedral is in thin lines. The seven-coordinated CaO_7 is outlined with dotted lines. Symmetry codes: a: $\frac{1}{2} - x, \frac{1}{2} + y, \frac{1}{2} - z$; b: $\frac{1}{2} - x, \frac{1}{2} - y, 1 - z$; c: $\frac{1}{2} - x, \frac{1}{2} - y, -z$; d: $1 - x, y, \frac{1}{2} - z$; e: $\frac{1}{2} + x, \frac{1}{2} - y, \frac{1}{2} + z$; f: $\frac{1}{2} - x, \frac{1}{2} - y, \frac{1}{2} - z$; g: $\frac{1}{2} + x, \frac{1}{2} - y, \frac{1}{2} + z$.

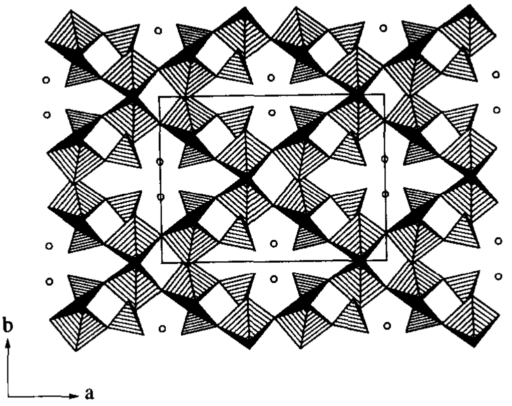

FIG. 2. A STRUPLO polyhedral plot of the structure of $CaNb_2P_2O_{11}$ is projected onto the *ab* plane. Ca atoms are shown as small circles. The unit cell boundaries are outlined by solid lines.

ing the terminal oxygen atoms, O(3), O(4), and O(5). The fourth phosphate oxygen atom, O(6), is found to be pointing away from the center of the Nb_4O_{20} unit. Four O(6) atoms, one from each phosphate group, together with one oxo oxygen, O(2), and two terminal oxygen atoms, O(4), form the seven–coordinated CaO_7, outlined by dotted lines in Fig. 1.

This mixed oxophosphate framework structure is projected onto the *ab* plane in a STRUPLO-86 polyhedral plot in Fig. 2 and shows the unit cell of $CaNb_2P_2O_{11}$. In the center of the plot, the previously defined Nb_4O_{20} unit is surrounded by eight PO_4 tetrahedra through the sharing of corner oxygen atoms to form a $[Nb_4P_8O_{44}]$ structural unit. Each structural unit shares all of its phosphate groups with four neighboring units to form an extended slab structure along the *ab* plane. Note that these structural units are centered around the inversion centers at $(0, 0, z)$ and $(\frac{1}{2}, \frac{1}{2}, z)$, where $z = 0$ or $\frac{1}{2}$ and propagate along the *c* axis to form an infinite $[Nb_4P_8O_{44}]_\infty$ unit. Furthermore, these infinite units are arranged forming channels along *c*.

An important structural feature of this compound rests on its infinite octahedral chains seen in the *bc* projection plane of Fig. 3. NbO_6 octahedra share corner oxygens in such a way that a double-layered, zig-zag chain is formed along [001]. Within a layer of NbO_6 octahedra (approximately in the *bc* plane), the octahedra share *cis* waist oxygen atoms, O(1). The interlayer atoms, between two stacked NbO_6 octahedral chains, are the shared apical oxygen atoms, O(2). Looking at the plane, one can see that the stacked NbO_6 octahedra are slightly staggered. The zig-zag formation of the chain, which dictates the shape of the channels, is a result of corner sharing *cis* oxygens by the NbO_6 octahedra. Because each niobium oxide chain is surrounded by PO_4 tetrahedra, as mentioned earlier, it can be regarded as an "isolated" unit. This chain is further separated from the neighboring chains, in the *bc*

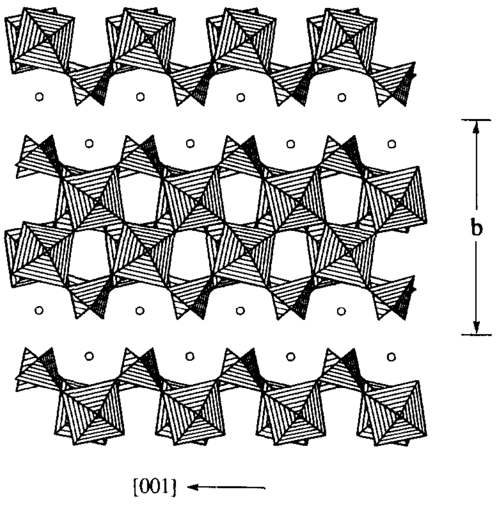

FIG. 3. The structure of $CaNb_2P_2O_{11}$ is drawn to show the mixed framework of the double-layered, zig-zag NbO_6 chains (propagating along [001]) and corner shared phosphate groups. Two identical slabs, one above and one below the plane (not drawn for clarity), are displaced by a half unit cell along *b* to form channel structures. The calcium atoms (small circles) are shown in the zig-zag channel structures. The unit cell dimension b is shown by the arrow bar.

TABLE III

SELECTED BOND DISTANCES (Å) AND ANGLES (deg) FOR THE NbO_6 OCTAHEDRON AND PO_4 TETRAHEDRON IN $CaNb_2P_2O_{11}$

NbO_6 Octahedron	
Nb-O(1)^a	1.856(3)
Nb-O(1)^b	1.922(3)
Nb-O(2)	1.931(1)
Nb-O(3)	1.971(3)
Nb-O(4)	2.164(3)
Nb-O(5)^c	2.009(3)
O(1)^a-Nb-O(1)^b	89.44(5)
O(1)^a-Nb-O(2)	94.3(1)
O(1)^a-Nb-O(3)	98.5(1)
O(1)^a-Nb-O(4)	172.1(1)
O(1)^a-Nb-O(5)^c	93.6(1)
O(1)^b-Nb-O(2)	97.3(1)
O(1)^b-Nb-O(3)	88.4 (1)
O(1)^b-Nb-O(4)	88.6(1)
O(1)^b-Nb-O(5)^c	174.3(1)
O(2)-Nb-O(3)	166.0(1)
O(2)-Nb-O(4)	78.4(1)
O(2)-Nb-O(5)^c	87.2(1)
O(3)-Nb-O(4)	89.1(1)
O(3)-Nb-O(5)^c	86.5(1)
O(4)-Nb-O(5)^c	89.0(1)
PO_4 Tetrahedron	
P-O(3)	1.544(3)
P-O(4)^b	1.539(3)
P-O(5)	1.539(3)
P-O(6)	1.513(3)
O(3)-P-O(4)^b	107.8(2)
O(3)-P-O(5)	108.1(2)
O(3)-P-O(6)	110.9(2)
O(4)^b-P-O(5)	110.1(2)
O(4)^b-P-O(6)	111.4(2)
O(5)-P-O(6)	108.4(2)

Note. See Fig. 1 for symmetry codes.

plane, by channels containing the calcium cations. Essentially, the channel can be viewed as being encompassed by four isolated chains, resulting from the stacking of two identical planes that are displaced by half an unit cell along *b* (one on the top and bottom of the *bc* plane).

The bond distances and angles for the NbO_6 octahedron are given in Table III. The three shorter distances (1.856 ~ 1.931 Å) correspond to the Nb–O bonds between NbO_6 octahedra, while the three longer bond lengths (1.971 ~ 2.164 Å) correspond to the Nb–O–P bridging bonds. The calculated valence sum (based upon the observed Nb–O distances and the formula suggested by Brown and Altermatt (*9*)) for the niobium cation is in a good agreement with the formal pentavalent oxidation state, e.g., 5.20 vs 5.00, respectively. Deviation of the octahedral bond angles indicates that the NbO_6 octahedron is slightly distorted. Both the NbO_6 octahedra and the PO_4 tetrahedra exhibit typical bond distances and angles as seen previously in niobium phosphate compounds (*4*). As for the PO_4 tetrahedra, the shortest P–O bond (1.513 Å compared to 1.539 ~ 1.544 Å) is associated with the unshared, phosphate oxygen atom, O(6).

The electrostatic interactions between the electropositive cation, calcium in this case, and the oxygen atoms are quite diverse. This is attributed to the differences in bonding nature with respect to the individual oxygen atoms with pentavalent niobium and/or phosphorus atoms. That is to say that the stronger the Nb–O and/or P–O covalent bond is, the weaker the electrostatic interaction will be between the calcium cation and shared oxygen anions, and subsequently, the longer the Ca–O distances. Intuitively, the P–O bond is more covalent than the Nb–O bond, thus the calcium electrostatic interaction should be weaker with the phosphorus-associated oxygen atom. Evidently, the observed calcium–oxygen distances reflect the bonding nature (covalency) and coordination environment (terminal vs bridging) of the oxygen atom, i.e., Ca–O(4) > Ca–O(2) > Ca–O(6) (see Table IV) is in the same order as P–O(4)–Nb > Nb–O(2)–Nb > P–O(6). Nevertheless, the Ca–O distances are in the range of 2.34 ~ 2.53 Å, which is comparable with the sum, 2.46 Å, of the Shannon crystal radii of oxygen (1.26 Å) and seven-coordinated calcium (1.20 Å) atoms (*10*).

TABLE IV

CALCIUM TO OXYGEN DISTANCES IN THE CaO_7 CONFIGURATION

Ca–O(2)	2.473(4)
Ca–O(4)^d	2.527(3) (2×)
Ca–O(6)^{c,e}	2.342(3) (2×)
Ca–O(6)^{f,g}	2.375(3) (2×)

Note. See Fig. 1 for symmetry codes.

The structure of the title compound is closely related to that of the isotypic compound $BaNb_2P_2O_{11}$ (*5*). In Fig. 4a the stacking of the double-layered NbO_6 octahedra of $CaNb_2P_2O_{11}$ is viewed down the *b* axis. For comparison, Fig. 4b illustrates the structure of the isotypic compound $BaNb_2P_2O_{11}$ from the same perspective. In both structures, each NbO_6 octahedron shares corner oxygen atoms with three NbO_6 octahedra and three PO_4 tetrahedra, while each PO_4 tetrahedron has one unshared oxygen that points into the cavity holding the electropositive cations. Furthermore, both structures consist of double ReO_3-type NbO_6 octahedral chains that are capped by PO_4 tetrahedra. The NbO_6 octahedral chains are separated by electropositive cation-containing channels or cages. The corner-sharing chains of NbO_6 octahedra are directed along different axes in the two compounds resulting in a slightly different orientation of the octahedra within the layers. In $CaNb_2P_2O_{11}$, the NbO_6 octahedral chains share oxygens along the octahedral fourfold axis. In contrast, the sharing of NbO_6 octahedra in $BaNb_2P_2O_{11}$ occurs along the threefold axis, which results in a hexagonal unit cell. The coordination of the electropositive cations differs between the two structures, seven for Ca^{2+} and thirteen for Ba^{2+}, giving rise to infinite channels in $CaNb_2P_2O_{11}$, but for $BaNb_2P_2O_{11}$, the cavity can be better described as cages containing the Ba cation.

Finally, the structure of the title compound resembles that of the quasi-low-dimensional structure frequently seen in the bronzes. In contrast to the double-layered,

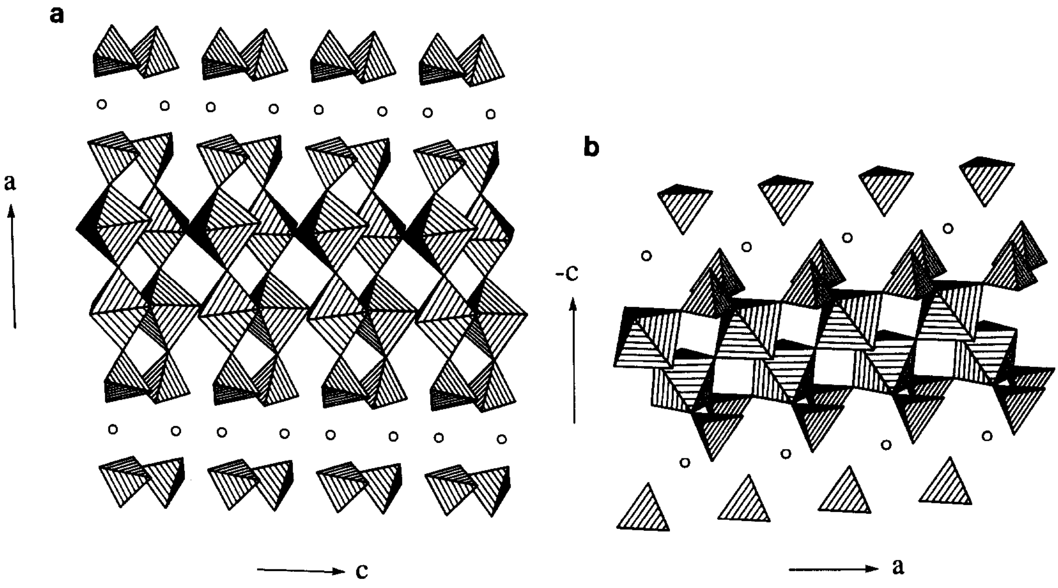

FIG. 4. The structures of (a) $CaNb_2P_2O_{11}$ and (b) $BaNb_2P_2O_{11}$ are shown from the same perspective view. The open circles represent the calcium and barium atoms, respectively.

isolated oxo frameworks observed in the previously discussed oxophosphate structures, $K_{0.9}Mo_6O_{17}$ (*6*) contains infinite two-dimensional slabs of corner-sharing MoO_6 octahedra that are four layers thick. As observed in $CaNb_2P_2O_{11}$, these slabs are also terminated on either side by a layer of corner-sharing MoO_4 tetrahedra, instead of PO_4 tetrahedra, and are accompanied by a layer of K^+ cations which separate the slabs. Consequently, the slabs are interrupted in the direction perpendicular to the octahedral conducting plane. As was discussed for $CaNb_2P_2O_{11}$ and $BaNb_2P_2O_{11}$, incorporation of a layer of closed-shell phosphate groups allows structurally isolated quasi-low-dimensional compounds to form. If the two isotypic niobium (V) oxophosphate compounds can be reduced, their structure type may provide a more electronically shielded oxide lattice for the study of the behavior of conducting electrons in a confined space. Presently, cation substitution reactions with a trivalent electropositive cation are underway.

Acknowledgments

Acknowledgment is made to the National Science Foundation, Solid State Chemistry (SGER), Grant DMR-9012983, and, in part, to the Petroleum Research Fund, administered by the ACS, for support of this research (Grant ACS-PRF 21154-G3). D.L.S. is indebted to the Dow Chemical Co. (1990–1991) and the Wray Trust (1991–1992) for fellowships. Financial support for the single crystal X-ray diffractometer by the National Science Foundation is gratefuly acknowledged.

References

1. J. B. Goodenough, *in* "Progress in Solid State Chemistry" (H. Russ, Ed.), Vol. 5, p. 145, Pergamon, Elmsford, NY (1971).
2. J. A. Wilson, *Adv. Phys.* **21,** 507 (1967).
3. M. Greenblatt, *Chem. Rev.* **88,** 31 (1988).
4. D. L. Serra and S.-J. Hwu, in preparation.
5. E. V. Murashova, V. K. Trunov, and Y. A. Velikodnyi, *Russ. J. Inorg. Chem.* **31,** 951 (1986).
6. J.-M. Reau, C. Fouassier, and P. Hagenmuller, *J. Solid State Chem.* **1,** 326 (1970).
7. "TEXSAN: Single Crystal Structure Analysis software, version 5.0," Molecular Structure Corp., The Woodlands, TX (1989).
8. G. M. Sheldrick, *in* "Crystallographic Computing 3" (G. M. Sheldrick, C. Krüger, and R. Goddard, Eds.), pp. 175–189, Oxford Univ. Press, London/New York (1985).
9. I. D. Brown and D. Altermatt, *Acta. Crystallogr., Sect. B: Struct. Sci.* **B41,** 244 (1985).
10. R. D. Shannon, *Acta Crystallogr., Sect. A: Cryst. Phys. Diffr. Theor. Gen. Crystallogr.* **A32,** 751 (1976).